Supplementary Materials:
Mediterranean Sea heat uptake variability as a precursor to winter precipitation in the Levant

Ofer Cohen[1], Assaf Hochman[1], Ehud Strobach[2], Dorita Rostkier-Edelstein[1,3], Hezi Gildor[1], and Ori Adam[1]

[1]The Hebrew university of Jerusalem, Jerusalem, Israel
[2]Agricultural Research Organization, Volcani Institute, Rishon LeTsiyon, Israel
[3]Holon Institute of Technology, Holon, Israel

Correspondence: Ori Adam (ori.adam@mail.huji.ac.il)

1 SOM analysis optimization

The SOM algorithm is used for projecting high-dimensional input data onto a lower-dimensional grid (typically two-dimensional). As the input data is presented to the SOM network, the algorithm identifies the Best Matching Unit (BMU), which is the node (or neuron) on the grid whose weight vector most closely resembles the input data. The SOM network then adjusts the weight vectors of the BMU and its neighboring nodes to better match the input data. This iterative process of competitive learning continues until the SOM stabilizes after the training epochs are over, clustering similar data points together and preserving the topological relationships of the input space.

We manually optimize the parameters used in the SOM analysis to maximize the correlation between the derived spatial patterns and Levant precipitation while trying to minimize the overall number of patterns. Specifically, we experiment with different network configurations looking for patterns identified by SOM that are statistically robust. The final parameters used in our SOM analysis are detailed in Table S1. Furthermore, the resulting SOM patterns are analyzed to discern their spatial characteristics and temporal frequency, as well as the temporal variance they explain (Figures 2 and 3 in the main text).

Parameter description	**Value**
Number of rows	1
Number of columns	3
Neighborhood function	Epanechnikov (ep)
Number of rough training iterations	5
Number of fine-tune training iterations	30
Neighborhood function initial radius	3
Neighborhood function final radius	1
Weight during mapping	2
Initialization scheme	Linear

Table S1. Parameters used in the SOM analysis.

2 Decomposition of Q_f SOM patterns

Figure S1 shows the changes in upper-ocean heat uptake (Q_f) during August (for which lagged correlations with Levant winter precipitation are strongest), associated with SOM Pattern 2 (Figure 3 in the main text), decomposed into downward surface latent and sensible heat fluxes, and downward shortwave and longwave radiation. Surface latent heat fluxes are seen to dominate Q_f anomalies during August, with a minor contribution from sensible heat flux, which spatially follows the latent heat flux anomalies, and negligible contribution by the radiative fluxes.

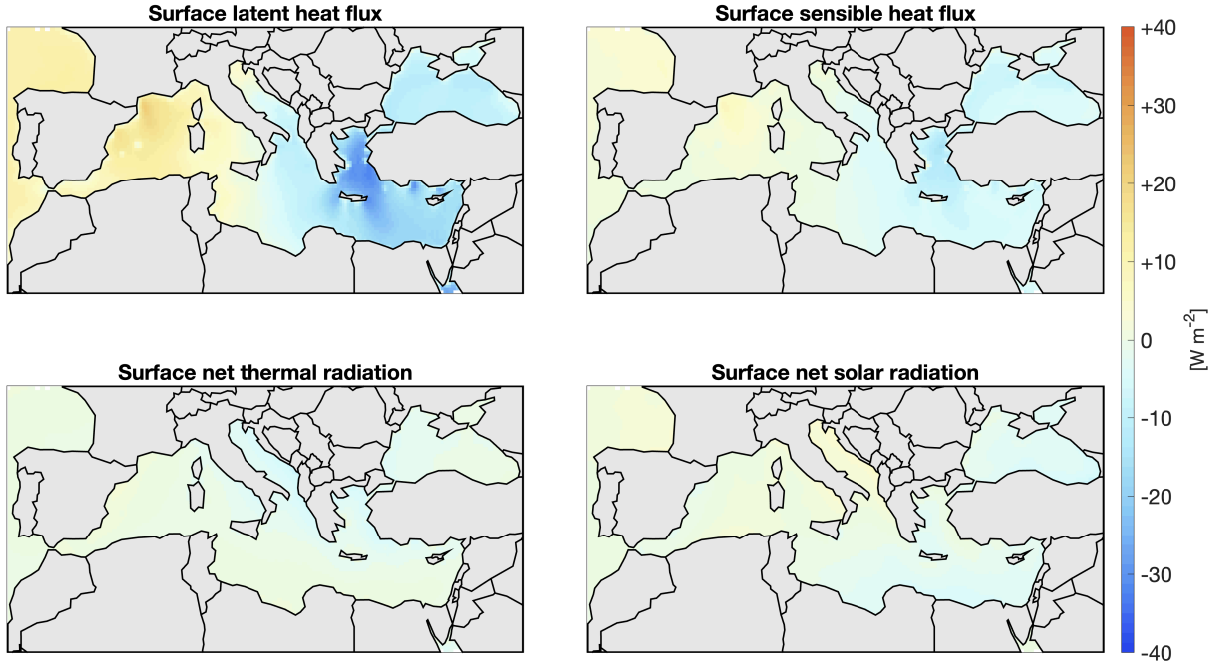

Figure S1. Decomposition of Q_f anomalies during August, associated with SOM Pattern 2 (Figure 3 in the main text) into downward: (**a**) latent heat fluxes, (**b**) sensible heat fluxes, (**c**) longwave radiation, and (**d**) shortwave radiation. Data taken from ERA5 during the period 1979–2023.

3 Extended AQA correlations to Levant winter precipitation

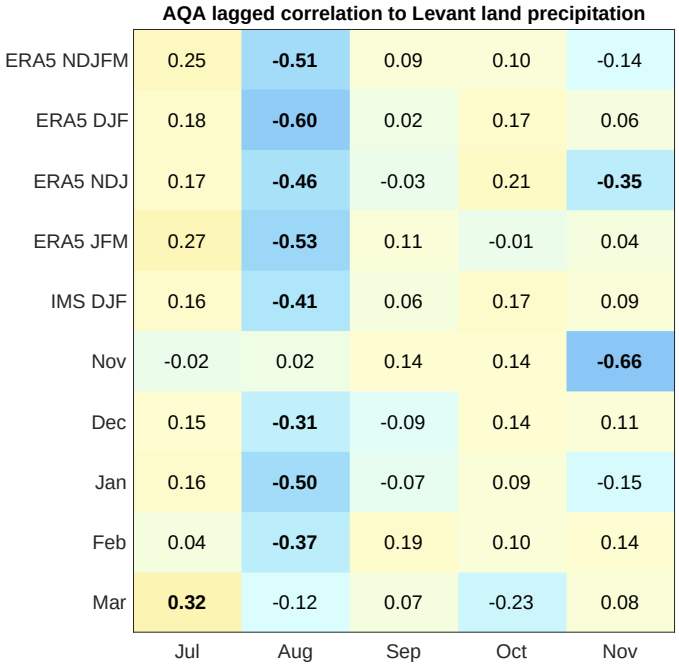

Figure S2. Correlations of AQA with Levant winter land precipitation for the months November–March, extending the lagged correlations shown in Figure 5b of the main text.

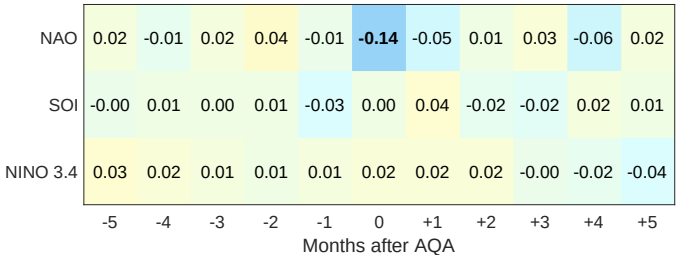

Figure S3. Lagged correlation of AQA and the North Atlantic Oscillation index (NAO), Southern Oscillation index (SOI), and SST anomaly in the NINO 3.4 region (NINO 3.4 index). NAO, SOI, and SST anomalies at NINO 3.4 were downloaded from *https://www.ncei.noaa.gov/access/monitoring/products/*. Based on index data availability, monthly NAO and SOI correlations are calculated for the period 1979–2023; and NINO 3.4 correlations calculated for the period 1982–2023.

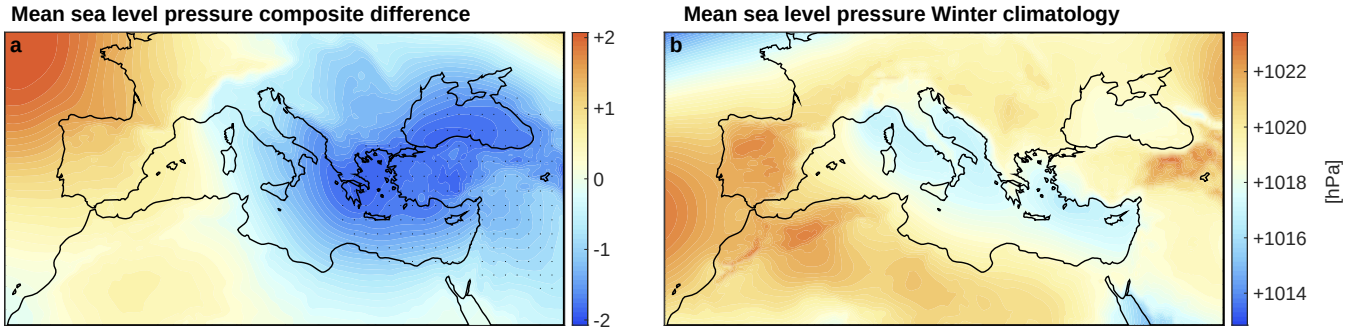

Figure S4. (a) Difference in monthly mean sea-level pressure during winter (Dec–Feb) between negative and positive AQA composites (i.e., AQA negative and positive values during the August preceding winter months). (b) The climatological mean winter mean sea-level pressure. Data taken from ERA5 for the years 1979–2023. Stippling indicates 95% confidence estimated using bootstrap.

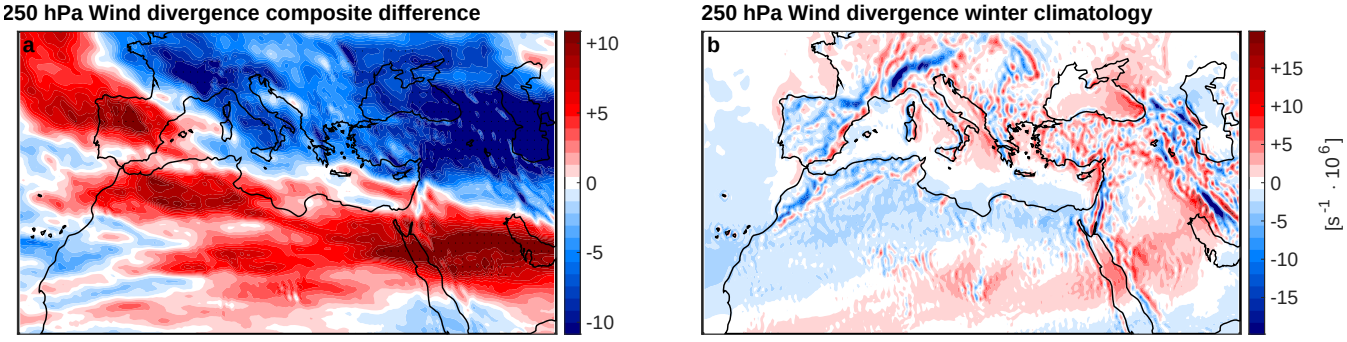

Figure S5. Wind divergence at the 250 hPa level. (a) Difference in 250 hPa wind divergence during winter (Dec–Feb) between negative and positive AQA composites (i.e., AQA negative and positive values during the August preceding winter months). (b) The climatological mean 250 hPa wind divergence during winter. Data taken from ERA5 for the years 1979–2023. Stippling indicates 95% confidence estimated using bootstrap.